Non-neutral plasma shapes and edge profiles

A. J. Peurrung and J. Fajans
Department of Physics, University of California, Berkeley, Berkeley, California 94720

(Received 25 July 1989; accepted 27 December 1989)

Non-neutral plasma shapes and edge profiles are investigated for various plasma and trap parameters. The equilibrium plasma shape is found numerically and compared to the analytically predicted shape. Special attention is given to the profile at the plasma end.

I. INTRODUCTION

Interest in non-neutral plasmas is steadily increasing. Non-neutral plasmas are unusually stable and quiescent; pure electron plasmas have been confined for longer than 40 000 sec, and densities of 5×10^{10} cm^{-3} have been achieved. Applications of these plasmas currently include basic plasma physics research, positron research, nuclear physics targets, low-temperature plasmas, and highly correlated plasmas.[1]

Many experiments use traps similar to the one shown in Fig. 1. The cylindrically symmetric plasma is trapped inside a series of gate cylinders. Radial confinement is provided by an axial magnetic field. Axial confinement is guaranteed by appropriately biasing the end gates. The shape of the plasma in the trap depends on the system parameters—specifically on the plasma density, radius, and temperature, and on the externally imposed electric fields that axially confine the plasma. Experiments often rely on exact knowledge of the plasma density. Frequently, however, only the density integrated along field lines is measured directly; knowledge of the plasma shape is required to construct the volume density.[2,3] Prasad and O'Neil studied the finite length global thermal equilibrium of non-neutral plasmas.[4] The problem of equilibria in a slab geometry is explored by Turner.[5] The plasmas considered in this paper need only be in equilibrium along individual field lines; they are not required to be in global thermal equilibrium. Equilibrium along individual field lines is attained far sooner than global thermal equilibrium.

Very cold plasmas in global thermal equilibrium have uniformly dense interiors. Changes in the plasma density occur only near the plasma surface, and have a scale length approximately equal to the Debye length. Many plasmas, however, are not well described by this cold, global thermal equilibrium limit. Because cross-field transport occurs slowly compared to motion along a field line, plasmas are often in a state of local thermal equilibrium, in which the plasma density follows a Boltzmann distribution along axial magnetic field lines.[3,6] Plasmas in local thermal equilibrium may fall off axially with a Debye scale length, but need not fall off radially with this scale length.

In general, the plasma reacts to changes in the vacuum potential by changing its density or its radius, or occasionally both simultaneously. As shown in Table I, plasmas can be placed into one of three categories. First, we divide plasmas into "thin" plasmas and "thick" plasmas according to whether the voltage drop across the plasma is less than or greater than the plasma temperature. If the voltage drop is greater than the temperature at the plasma end the plasma tends to adjust its radius; if the voltage drop is less than the temperature, the plasma adjusts its density. This division is equivalent to comparing the radius of the plasma to its Debye length. Note that thin plasmas are not true plasmas because collective effects are of little importance. Second, we further divide thick plasmas into two groups depending on the ratio of the interior plasma potential to the confining gate potential. (The interior plasma potential is the potential between the grounded storage gate and the plasma center, well away from the plasma end.) Plasmas whose interior potential is just less than the gate potential are close to escaping, and are designated "ill confined"; plasmas whose interior potential is much less than the gate potential are designated "well confined." Ill-confined plasmas have a neck that extends into the confining cylinders, while well-confined plasmas have a squared off end. At the extreme end of ill-confined plasmas, the local plasma radius will necessarily become small enough that the plasma will behave as a thin plasma.

II. THEORY AND SIMULATIONS

The electric field potential inside the trap can be divided into two distinct parts: the gate potential Φ_g and the plasma potential Φ_p. The gate potential satisfies Laplace's equation with appropriate boundary conditions, namely,

$$\nabla^2\Phi_g(r,z)=0,\qquad \Phi_g(r_w,z)=V_g(z), \tag{1}$$

where $V_g(z)$ is the potential on the gate walls and r_w is the radius of the wall. The plasma potential Φ_p satisfies Poisson's equation with a grounded wall boundary condition:

$$\nabla^2\Phi_p(r,z)=-4\pi en(r,z),\qquad \Phi_p(r_w,z)=0, \tag{2}$$

where $n(r,z)$ is the local particle density and e is the particle charge. The unique self-consistent solution for the potential and the charge density inside the trap is found by assuming that the charges along each field line obey Boltzmann's relation:

$$n(r_0,z)\propto \exp[-e\Phi(r_0,z)/T], \tag{3}$$

where $\Phi=\Phi_p+\Phi_g$ is the total potential and T is the plasma temperature. The Boltzmann equation is normalized by assuming that either the total charge on a field line

 0899-8221/90/040693-07$02.00

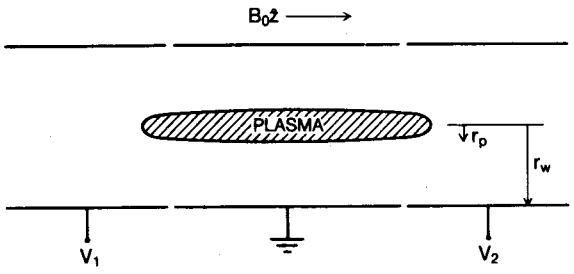

FIG. 1. Plasma confinement geometry. Axial confinement is achieved by appropriately biasing the end cylinders with voltages V_1 and V_2.

is known or that the density at some interior value of z is known. Although experimental data are often of the first type, we adopt the latter condition because it is numerically more convenient to work with a fixed central density. The same general types of behaviors are found for either condition.

If the plasma is sufficiently thin, hot, or tenuous, collective effects are unimportant. The plasma particles will closely conform to the gate potential Φ_g and the plasma shape will be largely determined by the external control voltages. In the opposite limit of thick, cold, and dense plasmas, collective effects are very important. Figure 2 shows the end shapes of three plasmas with different temperatures. In Fig. 2(a), the plasma is thin and the thermal energy is larger than the potential across the plasma. The charge at all radii reacts similarly to the gate voltage and the density contours are aligned with the gate potential contours. There is a gradual change in density and little change in radius. In Fig. 2(c), the plasma is thick and the potential across the plasma is larger than the temperature. Here the plasma radius shrinks gradually, but the interior density remains unchanged. In Fig. 2(b) the plasma parameters are intermediate between these two extremes, and the plasma profile adjusts by changing both its radius and its density. These distinctions are conveniently parame-

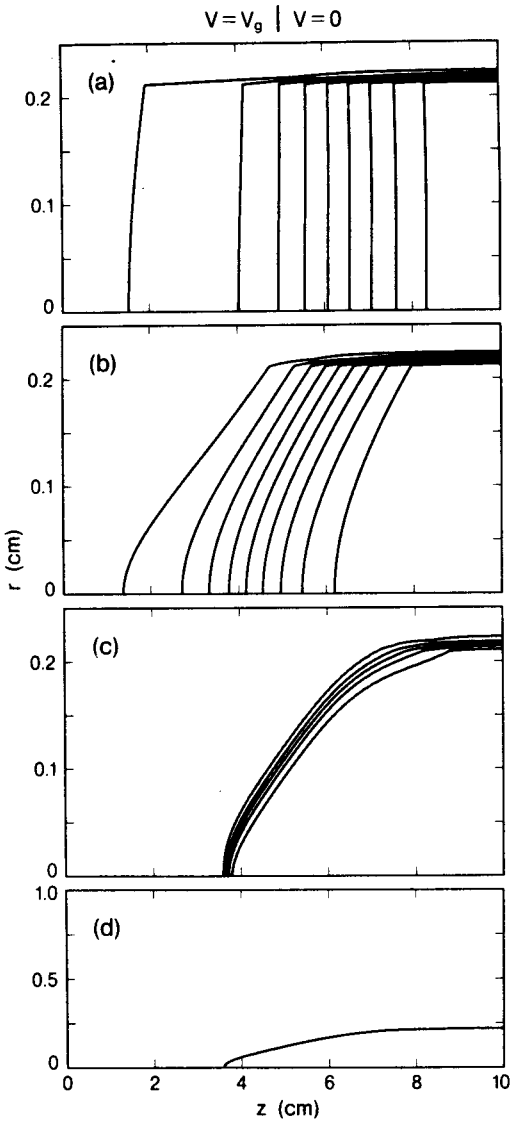

FIG. 2. Comparison of three plasma shapes with $n = 10^9$ cm^{-3}, $r_w = 2$ cm, and R values of (a) 0.036, (b) 3.6, and (c) 182. In (a) and (b) contours mark changes of 10% of the central density. In (c) contours mark changes of 20% of the central density. One contour (c) is shown in (d) with different axis scaling to give a clearer picture of the actual plasma shape. The transition between the biased end cylinder and the grounded central cylinder is shown at the top of (a).

TABLE I. Conceptual division of plasma types.

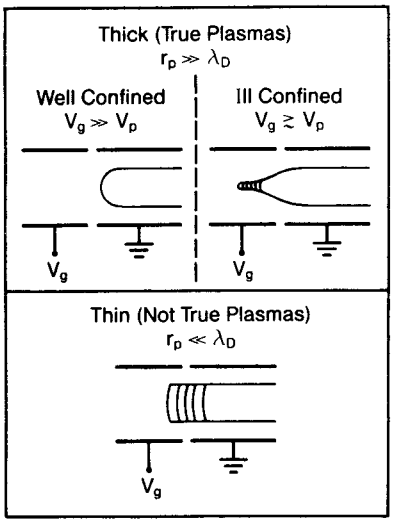

trized by R, the ratio of the potential across the plasma to the plasma temperature:

$$R = \pi r_p^2 n_0 e^2 / T = (r_p / 2\lambda_D)^2, \tag{4}$$

where r_p is the plasma radius well away from the plasma end and n_0 is the central density. Note that thin plasmas, defined by $R \ll 1$, do not satisfy one of the common conditions that define the plasma state, namely, that $r_p \gg \lambda_D$. Here $\lambda_D = (T/4\pi n_0 e^2)^{1/2}$ is the Debye length.

If $R \gg \frac{1}{4}$ and if $r_p \ll r_w$, then the plasma shape is largely determined by the degree of confinement, i.e., by the ratio of the potential at the center of the plasma to the maximum stopping potential. In Fig. 3, we show the plasma shape for three different gate voltages. The plasmas range from well

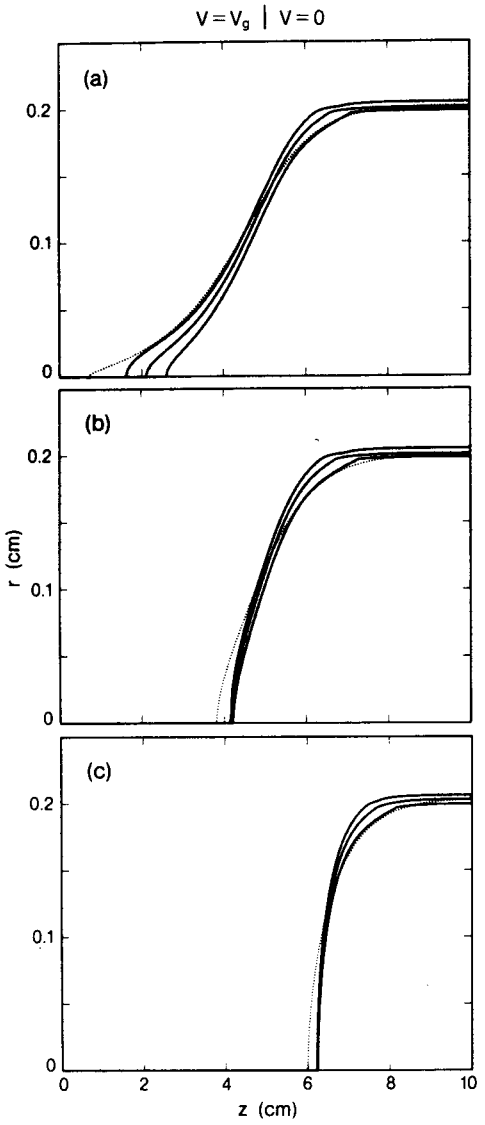

FIG. 3. Numerical (solid) and theoretical (dotted) shapes of a single plasma with $R = 182$ for three confinement voltages of (a) 104 V, (b) 125 V, and (c) 500 V. Solid lines mark 20%, 50%, and 80% of the central density.

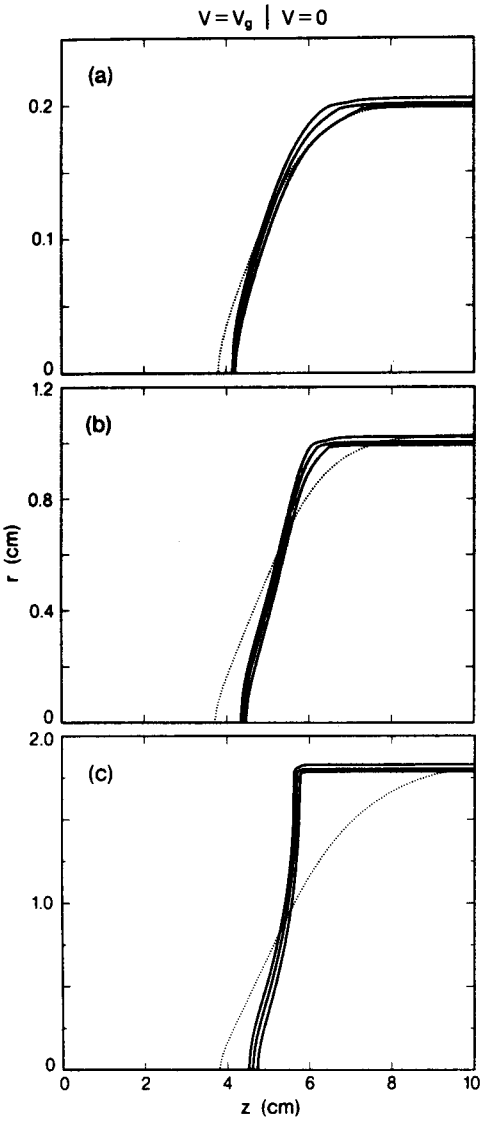

FIG. 4. Numerical (solid) and theoretical (dotted) shapes for plasmas with $R = 182$ and (a) $r_p/r_w = 0.1$, (b) $r_p/r_w = 0.5$, and (c) $r_p/r_w = 0.9$. Solid lines mark 20%, 50%, and 80% of the central density. The confinement voltage and density are chosen so that the plasma ends at the same axial position.

to ill confined with $r_p/r_w = 0.1$ and $R = 182$. For the most ill-confined plasma, Fig. 3(a), the interior plasma potential $V_p = 103.44$ V is almost equal to the confining gate voltage $V_g = 104$ V, and the plasma protrudes well into the confining gate. For V_g sufficiently close to V_p, the plasma will end near the position of the voltage maximum in the confining gate (normally, but not always, in the center of the confining gate).

For plasma radii r_p well less than wall radii r_w, we find that for constant V_g and V_p the plasma shape is roughly independent of r_p. Only when r_p is comparable to r_w do the off-axis components to the external gate fields greatly affect the plasma shape. In Fig. 4, we show the shape for an ill-confined plasma for three values of r_p.

We have routinely simulated plasmas with R values as high as 450. For a density of 10^9 cm^{-3} and a radius of 0.1 cm, this limit corresponds to a plasma temperature of 0.01 eV. The plasma profiles are found iteratively; Poisson's equation is used to find the electric fields from an assumed density distribution, and then the charge is redistributed along field lines according to the Boltzmann relation. These steps are repeated until adequate convergence is obtained. Unphysical numeric instabilities cause simulations of high density, low-temperature plasmas to converge very slowly, and, without careful control, slight density and potential errors grow rapidly. Unless the grid spacing inside the plasma is on the order of the Debye length or smaller, these instabilities will prevent adequate convergence. This algorithm, which we adapted for our numeric simulation, was originally developed by Prasad, and relies on a Poisson solver algorithm developed by Hughes.[7] We have modified

the Poisson solver algorithm to allow variable size grid spacing in the r direction. All simulations are run until further iterations do not significantly alter the plasma shape, and the numerical results presented here are independent of any change in the grid spacing.

In the limit of constant density thick plasmas $[\lambda_D \to 0, n(r,z) \to n_0]$, for which $r_p \ll r_w$, the plasma shape can be found analytically. We will assume that far from the confining gates, the on-axis plasma potential is V_p; the problem to be solved is to determine the local plasma radius $\rho(z)$, given a varying on-axis confinement gate potential $\Phi_g(z)$. In the Appendix we demonstrate that potential of a plasma of variable radius is approximately

$$\Phi_p(r,z) = \begin{cases} 2\pi n_0 e \rho^2 \ln\left(\dfrac{r_w}{r}\right), & r > \rho, \\ 2\pi n_0 e \rho^2 \left[\ln\left(\dfrac{r_w}{\rho}\right) + \dfrac{1}{2}\left(1 - \dfrac{r^2}{\rho^2}\right)\right], & r < \rho, \end{cases} \tag{5}$$

where $\rho(z)$ is the sought after function describing the plasma shape. This approximation is most accurate when the plasma is narrow compared to the wall radius, and its radius changes sufficiently slowly with z.

On the $r = 0$ axis, Eq. (5) reduces to

$$\Phi_p(z) = 2\pi n_0 e \rho^2 [\ln(r_w/\rho) + \tfrac{1}{2}]. \tag{6}$$

The Boltzmann condition assures that the potential along field lines is constant inside the plasma. As shown above, the plasma meets this condition by varying its local radius $\rho(z)$. Thus the total potential must be constant along the $r=0$ axis:

$$\begin{aligned} V_p &= \Phi_g(z) + \Phi_p(z) \\ &= \Phi_g(z) + 2\pi n_0 e \rho^2 [\ln(r_w/\rho) + \tfrac{1}{2}], \end{aligned} \tag{7}$$

where V_p is the value of the total potential at the plasma center. This equation is easily solved for $\rho(z)$, to wit

$$\rho^2 [\ln(r_w/\rho) + \tfrac{1}{2}] = (1/2\pi n_0 e)[V_p - \Phi_g(z)]. \tag{8}$$

As shown in Figs. 3 and 4, the solution of Eq. (8) is often in close agreement with the numeric simulations. For $\rho \approx r_w$, however, the agreement is not nearly as good [Fig. 4(c)]. Since this analytic method is much faster than simulations (seconds instead of days, in the extreme), it should be employed whenever possible. Although we are unable at this time to numerically simulate off-axis plasmas, we speculate that the analytic method given here could be easily adapted to finding the shapes of such plasmas.

III. EDGE BEHAVIOR

As expected, we find that all thick plasmas have interior densities independent of z;all density variations occur near the plasma edge. In addition, all of the edge density profiles are qualitatively similar, differing only in the length scale for the dropoff. Most plasmas exhibit three fundamentally different types of edge behavior. First, well away from the plasma end, the plasma surface extends normal to the radial direction. The edge behavior here is

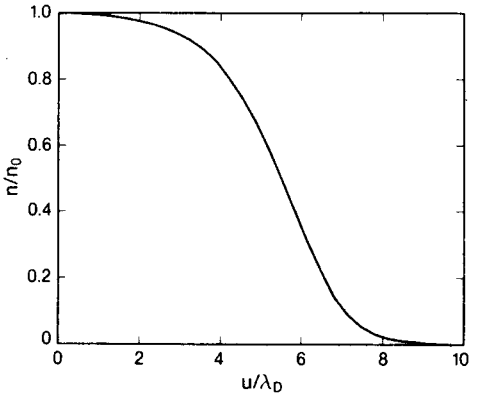

FIG. 5. The density field at the edge of the plasma, near its ends, as a function of distance perpendicularly outward from the plasma surface.

governed by slow cross-field transport, which eventually causes the plasma to approach global thermal equilibrium. Rather than model this extremely complicated process, we simply choose the radial density profile to be physically reasonable. Second, at the extreme tips of the plasma where the plasma radius is almost zero, the plasma is technically thin ($R \ll 1$) and requires numerical treatment. Finally, the plasma away from the extreme tip, but not yet in the bulk of the plasma, can be treated analytically. The edge thickness in this region is on the order of the Debye length.

Figure 5 shows the density as a function of u, the distance outward normal to the plasma surface for a thick plasma. Numerically, it is found that the density near the plasma ($n > n_0/2$) can be modeled as

$$n = n_0(1 - e^{u/L}), \tag{9}$$

while outside the plasma ($n < n_0/3$) the dependence becomes

$$n \propto n_0 \exp[-(u - u_0)^2/2L^2]. \tag{10}$$

For plasmas in global thermal equilibrium, these relations are in agreement with the "universal function" of Ref. 4. The numerically obtained results shown in Fig. 5, however, are not restricted to plasmas in global thermal equilibrium. All that is required is that the plasma be in local thermal equilibrium along a magnetic field line. In Fig. 6, Eqs. (9) and (10) are used to determine the scale length L for plasmas with varying degrees of confinement and various Debye lengths. We find that away from the extreme tip the length L is approximately equal to the Debye length and is independent of the confining voltage. At the extreme tip, however, the length L scales with both the Debye length and the degree of plasma confinement. For well-confined plasmas L approaches the Debye length, but for ill-confined plasmas L can be many times greater than the Debye length. [Note that Fig. 3(a) shows a typical ill-confined plasma.]

If we assume that the plasma potential is well modeled by Eq. (5), then we can find an analytical form for the density falloff away from the plasma interior. Our argu-

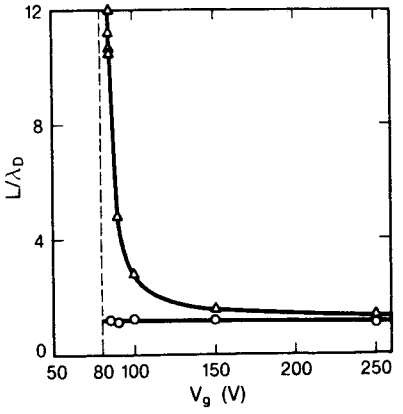

FIG. 6. Falloff distance near the plasma tip (triangles) and away from the tip (circles) as a function of confinement voltage. All falloff distances scale with the Debye length. The plasma escapes when V_g is lowered below 80 V.

ment requires only that the plasma be in local thermal equilibrium, not global thermal equilibrium. To find the total potential we assume that the plasma has an abrupt edge at r_p, which changes by an amount δr as a result of the change in gate potential with z. Figure 7 shows the geometry for this calculation. Since by assumption $\Phi_g(b) = \Phi_g(d)$, we find from Eq. (5) that

$$\Phi(b) - \Phi(d) = 2\pi n_0 e r_p^2 \left(\frac{1}{2} + \ln \frac{r_w}{r_p} - \ln \frac{r_w}{r_p + \delta r} \right). \tag{11}$$

Similarly,

$$\Phi(c) - \Phi(f) = \pi n_0 e (r_p + \delta r)^2. \tag{12}$$

Since voltage is constant along field lines inside the plasma we have $\Phi(b) = \Phi(c)$. Then the potential difference between two points of the same radius but at different z and with different gate potentials is

$$\Phi(d) - \Phi(f) = 2\pi n_0 e (\delta r)^2 + O[(\delta r)^3]. \tag{13}$$

Using the Boltzmann equation, Eq. (3), we can solve for the density dependence:

$$n(r) \propto \exp\left(\frac{-e[\Phi(d) - \Phi(f)]}{T} \right) = \exp\left(-\frac{(r - r_p)^2}{2\lambda_D^2} \right). \tag{14}$$

By comparing this result with Eq. (10), we conclude that L can be identified as the Debye length. Although here we assume a constant density in the interior of the plasma, our argument could easily be adapted to more complicated radial density profiles.

Because the potential far from the plasma edge is independent of the detailed form of the density dropoff, Eq. (14) accurately describes the density profile far outside the plasma. Since away from the plasma tip the normal to the plasma surface is nearly in the radial direction, Eq. (14) agrees with the numerically observed dropoff of Eq. (10). The approximations used to derive this result break down when $\delta z \approx \delta r$, i.e., when the plasma radius is changing rapidly. However, this happens only at the plasma's extreme tip, where the plasma shape has necked down to $r_p \lesssim 2\lambda_D$. Here $R \ll 1$, and the plasma will begin to adjust its density instead of its shape. The density will be given by the Boltzmann relation, with the controlling voltage approximately equal to the gate potential. For ill-confined plasmas, this narrow region occurs well inside the confining cylinder. Because the gate potential here varies slowly, the density falloff is similarly slow. Thus the density falloff can occur over many Debye lengths. For well-confined plasmas, however, the gate potential varies quickly, and the plasma scale length remains approximately equal to the Debye length.

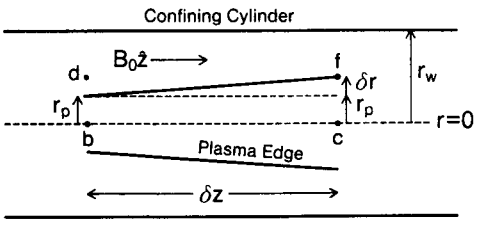

FIG. 7. Geometry for the edge profile calculation.

IV. CONCLUSION

In summary, we have examined the shapes and profiles of general non-neutral plasmas. These plasmas need only be in equilibrium along individual field lines. The shape assumed by a non-neutral plasma is determined largely by its value of R, its degree of confinement, and by its radius. For many experimentally relevant cases, where $R \gg 1$ and $r_p \ll r_w$, a simple analytic theory accurately predicts the plasma shape. Plasma edges governed by charge transport along field lines are normally several Debye lengths thick and have the form of the universal function shown in Fig. 5. However, the edge thickness at the tip of an ill-confined plasma exhibits a strong dependence on confining voltage.

ACKNOWLEDGMENTS

The computer program, which was modified for use in this work, was written by C. Driscoll, K. Fine, and S. Prasad. We have enjoyed useful discussions with B. Beck, K. Fine, and A. Hyatt. Some of this work was performed at the University of California, San Diego.

This work is supported by the National Science Foundation, the Miller Institute, and the Office of Naval Research.

APPENDIX: POTENTIAL FROM A ROD OF CHARGE

In this appendix we justify our expression [Eq. (5)] for the potential of a variable radius plasma. We will find the appropriate Green's function, perform the required convolution integral, and show that for many plasmas the potential is well approximated by Eq. (5). Finally we explicitly calculate the dominant error in Eq. (5) and show, via a numerical example, that the error is indeed small.

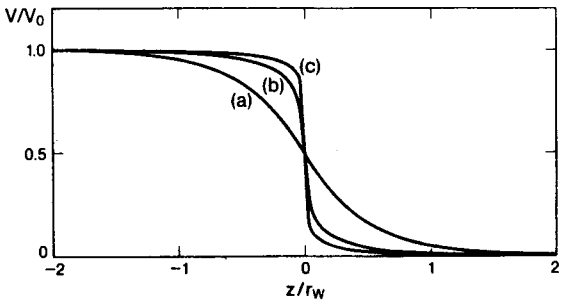

FIG. 8. On-axis potential near the end of a charged rod for (a) $r_p/r_w = 1.0$, (b) $r_p/r_w = 0.01$, (c) $r_p/r_w = 0.0001$. The rod extends from minus infinity and terminates abruptly at $z = 0$.

First we calculate the potential of a semi-infinite, constant density charged rod of radius r_p, extending from minus infinity to $z = 0$. Anticipating the result, in Fig. 8 we show the on-axis potential near the ends of several semi-infinite rods of different radius. Note that if the rod radius r_p is much less than the wall radius r_w, then the length scale of the potential dropoff near $z = 0$ is substantially less than the wall radius. Thus, when calculating the potential of a plasma with varying radius, only contributions from a small local neighborhood need be retained.

The potential of a semi-infinite charged rod of charge with radius r_p, density n, and extending from minus infinity to $z = 0$ and inside a grounded conducting wall at $r = r_w$, is given by the Fourier–Bessel series:

$$\Phi(r,z) = \begin{cases} \Phi_{\text{inf}}(r) - \sum_k D_k J_0\left(\frac{\chi_k r}{r_w}\right)\exp\left(\frac{\chi_k z}{r_w}\right), & z<0, \\ \sum_k D_k J_0\left(\frac{\chi_k r}{r_w}\right)\exp\left(\frac{\chi_k z}{r_w}\right), & z>0, \end{cases} \tag{A1}$$

where J_0 is a Bessel function of the first kind, χ_k are the Bessel function zeros satisfying $J_0(\chi_k) = 0$, and D_k are unknown coefficients. The infinite length rod potential Φ_{inf} is

$$\Phi_{\text{inf}}(r) = \begin{cases} 2\pi n e r_p^2 \ln\left(\frac{r_w}{r}\right), & r>r_p, \\ 2\pi n e r_p^2\left[\ln\left(\frac{r_w}{r_p}\right) + \frac{1}{2}\left(1-\frac{r^2}{r_p^2}\right)\right], & r<r_p. \end{cases} \tag{A2}$$

The Fourier–Bessel series automatically satisfies all the wall boundary conditions and the $z = 0$ derivative matching condition. The coefficients, D_k, are determined by matching the solutions for $z<0$ and $z>0$ across the $z=0$ boundary, and thus

$$\sum_k D_k J_0\left(\frac{\chi_k r}{r_w}\right) = \begin{cases} \pi n e r_p^2 \ln\left(\frac{r_w}{r}\right), & r>r_p \\ \pi n e r_p^2\left[\ln\left(\frac{r_w}{r_p}\right) + \frac{1}{2}\left(1-\frac{r^2}{r_p^2}\right)\right] & r<r_p \end{cases} . \tag{A3}$$

Multiplying both sides by $rJ_0(\chi_k r/r_w)$ and integrating from 0 to r_w eventually yields the coefficients D_k:

$$D_k = \frac{4\pi n e r_p r_w}{\chi_k^3}\frac{J_1(\chi_k r_p/r_w)}{J_1^2(\chi_k)}. \tag{A4}$$

By adjusting the density so that $n = V_p/\{2\pi e r_p^2[\frac{1}{2} + \ln(r_w/r_p)]\}$, we fix the voltage, V_p, at the center of the rods. Thus the potential dropoff for $z>0$, as shown in Fig. 8, is

$$\Phi_{z>0}(r=0,z) = \frac{2V_p r_w}{r_p(\frac{1}{2}+\ln r_w/r_p)} \times \sum_k \frac{J_1(\chi_k r_p/r_w)}{\chi_k^3 J_1^2(\chi_k)}\exp\left(\frac{-\chi_k z}{r_w}\right). \tag{A5}$$

For narrow plasmas this further simplifies to

$$\Phi_{z>0}(r=0,z) = \frac{2V_p r_w}{r_p \ln r_w/r_p}\sum_k \frac{J_1(\chi_k r_p/r_w)}{\chi_k^3 J_1^2(\chi_k)}\exp\left(\frac{-\chi_k z}{r_w}\right). \tag{A6}$$

It can be shown that this dropoff contains roughly equal contributions from all length scales between the radius of the rod and the radius of the wall. Consequently the dropoff approaches an idealized step function when the radius of the plasma approaches zero (see Fig. 8).

Next we rewrite Eq. (A1), the potential of the semi-infinite charged rod, as the sum of two distinct parts,

$$\Phi(r=0,z) = u(-z)\Phi_{\text{inf}}(r) + \Phi_{\text{err}}(z), \tag{A7}$$

where $u(z)$ is the unit step function, $\Phi_{\text{inf}}(r)$ is the infinite rod potential, and $\Phi_{\text{err}}(z)$ is the difference between the actual solution and the step function idealization. If only the step function term in Eq. (A7) is kept, the Green's function is obvious (a delta function) and the convolution of this Green's function leads immediately and exactly to Eq. (5). [Note that the convolution is with a constant density disk of radius $\rho(z)$.] The error incurred by using Eq. (5) to approximate the plasma potential is solely due to $\Phi_{\text{err}}(z)$. This error is found by forming the Green's function corresponding to Φ_{err}. Carefully accounting for the change in sign at $z = 0$, the Green's function is found by differentiating $\Phi_{\text{err}}(-z)$:

$$G_{\text{err}}(z',z;\rho) = \sum_k \frac{4\pi n e \rho(z') J_1[\chi_k \rho(z')/r_w]}{\chi_k^2 J_1^2(\chi_k)} \times \exp\left(\frac{-\chi_k|z'-z|}{r_w}\right) - V_\infty[\rho(z)]\delta(z'-z), \tag{A8}$$

where $\rho(z)$ is the local, varying plasma radius and $V_\infty(r)$ is the axis voltage of an infinite length rod of plasma of radius ρ.

The correction to the potential in Eq. (5), Φ_{err}, is given by the convolution integral

$$\Phi_{\rm err}(z) \approx -V_\infty[\rho(z)] + \sum_k \frac{2\pi ne}{\chi_k r_w J_1^2(\chi_k)} \int_{-\infty}^{\infty} \rho^2(z') \times \exp\left(\frac{-\chi_k|z'-z|}{r_w}\right) dz', \tag{A9}$$

where we have used the approximation that $J_1[\chi_k \rho(z')/r_w] \approx \chi_k \rho(z')/2r_w$. This expression can be simplified by canceling the first term with the zeroth-order contribution from the integral:

$$\Phi_{\rm err}(z) \approx \sum_k \frac{2\pi ne}{\chi_k r_w J_1^2(\chi_k)} \int_{-\infty}^{\infty} [\rho^2(z') - \rho^2(z)] \exp\left(\frac{-\chi_k|z'-z|}{r_w}\right) dz'. \tag{A10}$$

The above expression is generally valid and can be used to estimate the errors inherent in Eq. (5).

In order to provide a specific numerical example, we use Eq. (8) to express the plasma radius in terms of the gate potential. Assuming for simplicity that the plasma is poorly confined [$V_p \approx \Phi_g(-\infty)$] gives the result

$$\Phi_{\rm err}(z) \approx \sum_k A_k \int_{-\infty}^{\infty} [\Phi_g(z) - \Phi_g(z')] \times \exp\left(\frac{-\chi_k|z'-z|}{r_w}\right) dz,' \tag{A11}$$

with

$$A_k = \{\chi_k r_w J_1^2(\chi_k)[\ln(r_w/\tilde{\rho}) + \tfrac{1}{2}]\}^{-1},$$

and where we have approximated the plasma radius as $\tilde{\rho}$ inside the logarithm. As expected, we find that the error as $[\ln(r_w/\tilde{\rho})]^{-1}$.

To proceed, we approximate the $r=0$ vacuum potential as

$$\Phi_g \approx \begin{cases} \frac{1}{2}V_p \exp(\chi_1 z/r_w), & z<0, \\ V_p[1-\frac{1}{2}\exp(-\chi_1 z/r_w)], & z>0, \end{cases} \tag{A12}$$

where V_g is the confining wall voltage. Carrying out the integration in Eq. (A11) and assuming each term separately attains its maximum value yields the result

$$\Phi_{\rm err} \approx 0.06 V_p,$$

for a plasma with $r_p/r_w = 0.1$ and a central voltage V_p far from the plasma ends. Although the magnitude of $\Phi_{\rm err}$ can be larger for well-confined plasmas, the rapidly changing gate potential causes this greater error to have little impact on the plasma shape. We conclude, therefore, that as long as $\tilde{\rho}/r_w \ll 1$, Eq. (5) accurately approximates the true plasma potential.

[1] J. H. Malmberg, C. F. Driscoll, B. Beck, D. L. Eggleston, J. Fajans, K. Fine, X. P. Huang, and A. W. Hyatt, in *Non-Neutral Plasma Physics*, AIP Conf. Proc. No. 175 (American Institute of Physics, New York, 1988), p. 28; and other articles therein.

[2] T. M. O'Neil, C. F. Driscoll, and D. H. E. Dubin, in *Turbulence and Anomalous Transport in Magnetized Plasmas* (Editions de Physique, Orsay, France, 1987), pp. 293–308.

[3] A. W. Hyatt, C. F. Driscoll, and J. H. Malmberg, Phys. Rev. Lett. **59**, 2975 (1987).

[4] S. A. Prasad and T. M. O'Neil, Phys. Fluids **22**, 278 (1979).

[5] L. Turner, Phys. Fluids **30**, 3196 (1987).

[6] C. F. Driscoll, J. H. Malmberg, and K. S. Fine, Phys. Rev. Lett. **60**, 1290 (1988).

[7] M. H. Hughes, Comput. Phys. Commun. **2**, 157 (1971).